Experimental and Monte Carlo Simulation Studies of the Thermodynamics of Polyethyleneglycol Chains Grafted to Lipid Bilayers

Sybille Rex,*# Martin J. Zuckermann,# Michel Lafleur,§ and John R. Silvius*
*Department of Biochemistry and #Department of Physics, McGill University, Montréal, Québec H3G 1Y6; and §Département de Chimie, Université de Montréal, Montréal, Québec H3C 3J7, Canada

ABSTRACT Experimental measurements of the affinity of binding of fluorescent acylated polyethyleneglycol (PEG) conjugates to bilayers containing varying levels of phosphatidylethanolamine-PEGs (PE-PEGs) have been combined with Monte Carlo simulations to investigate the properties of the polymer chains at a PEG-grafted lipid interface. The affinity of binding of such conjugates to large unilamellar phosphatidylcholine/phosphatidylethanolamine (9:1) vesicles decreases 27-fold as the size of the coupled PEG chain increases from 1 to 114 monomer units. Incorporation of increasing amounts of PE-PEG2000 or PE-PEG5000 into the vesicles progressively reduces the affinity of binding of acylpeptide-PEG2000 or -PEG5000 conjugates. Monte Carlo simulations of surfaces with grafted PEG chains revealed no significant dependence of several characteristic properties of the polymer chains, including the average internal energy per polymer and the radii of gyration, on the grafting density in the range examined experimentally. The average conformation of a surface-grafted PEG2000 or PEG5000 chain was calculated to be fairly extended even at low grafting densities, and the projected cross-sectional areas of the grafted PEG chains are considerably smaller than those predicted on the basis of the estimated Flory radius. The experimental variation of the binding affinity of acylated conjugates for bilayers containing varying mole fractions of PE-PEG2000 or -PEG5000 is well explained by expressions treating the surface-grafted PEG polymers either as a van der Waals gas or as a system of rigid discs described by scaled particle theory. From the combined results of our experimental and simulation studies we conclude that the grafted PEG chains exist in a "mushroom" regime throughout the range of polymer densities examined experimentally and that the diminished affinity of binding of acylated-PEG conjugates to bilayers containing PE-PEGs results from occlusion of the surface area accessible for conjugate binding by the mobile PE-PEG polymer chains.

INTRODUCTION

The reversible binding of macromolecules to natural and artificial membranes is a phenomenon of considerable importance in a variety of physiological and pharmacological contexts (Bongrand, 1988; Woodle and Lasic, 1992; Allen, 1992; Woodle et al., 1995; Lasic and Papahadjopoulos, 1995; Gregoriadis, 1995). The affinity of such interactions may be significantly affected by "crowding" of membrane surfaces due to the presence of biological or artificial macromolecules. Eukaryotic cellular membranes such as the plasma membrane may be covered on the extracytoplasmic side by a thick glycoprotein/glycolipid coat and on the cytoplasmic side by membrane-adsorbed proteins, cytoplasmic domains of transmembrane proteins, and juxtamembrane cytoskeletal elements. Steric interference by the surface-associated macromolecules may significantly affect the ability of other macromolecules to bind to the membrane surface. Liposomes bearing covalently coupled hydrophilic polymers such as polyethyleneglycols (PEGs) or dextrans have been shown to exhibit superior pharmacological properties compared to "bare" liposomes (Mori et al., 1991; Allen et al., 1991; Martin and Lasic, 1991; Woodle et al., 1991a,b; Lasic et al., 1991a, 1992; Blume and Cevc, 1993; Iga et al., 1994; Parr et al., 1994; Lasic, 1995). This phenomenon has been attributed to reduced binding of plasma macromolecules, including potential opsonizing factors, such as immunoglobulins and complement proteins, to the liposomal surface (Woodle and Lasic, 1992; Blume and Cevc, 1993; Woodle, 1993).

To better understand the nature and consequences of molecular crowding at a polymer-grafted membrane surface, we have combined experimental and simulation methods to examine the thermodynamics of polymer-polymer interactions in PEG-grafted lipid surfaces. Measurements of the affinity of binding of low levels of acylated PEGs to lipid vesicles containing varying densities of grafted PEG chains (POPE-polyethyleneglycols, PE-PEGs) have permitted us to probe the state of surface-grafted PEG chains as a function of the grafting density. The results of these experiments have been analyzed in the light of Monte Carlo (MC) simulations of the properties of PEG2000 and PEG5000 chains (PEGx, polyethyleneglycol of molecular weight x) bound to a planar surface at grafting densities comparable to those examined experimentally. Our experimental and MC simulation results, taken together, suggest that within the range of PE-PEG2000 or -PEG5000 contents normally used to generate "sterically stabilized" liposomes (0–10 mol% PE-PEG2000 or 0–6 mol% PE-PEG5000), the grafted chains do not undergo dramatic variations in average conformation, remaining within the "mushroom" as opposed

Received for publication 28 January 1998 and in final form 21 August 1998.

Address reprint requests to Dr. John R. Silvius, Department of Biochemistry, McGill University, Montreal University, Montreal, QC H3G 1Y6, Canada. Tel.: 514-398-7267; Fax: 514-398-7384; E-mail: silvius@med.mcgill.ca.

0006-3495/98/12/2900/15 $2.00

to the "brush" regime throughout this range of grafting densities.

MATERIALS AND METHODS

Materials

Egg yolk phosphatidylcholine (egg PC), 1-palmitoyl-2-oleoylphosphatidylethanolamine (POPE), 1-palmitoyl-2-oleoylphosphatidylglycerol (POPG), POPE-PEG2000, and POPE-PEG5000 were purchased from Avanti Polar Lipids (Alabaster, AL). *N*-Tris-[hydroxymethyl]methyl-2-aminoethanesulfonic acid (TES), HEPES, calcein, Triton X-100, bromobimane, palmitic and stearic acids, and monomethoxy-PEGs were obtained from Sigma Chemical Co. (St. Louis, MO), and Sephadex G-50 was from Pharmacia (Baie d'Urfe, Québec). Reagents for peptide synthesis were obtained from Novabiochem (La Jolla, CA), and ethanolamine was from Aldrich (Milwaukee, WI).

Acylpeptides acyl-GTCG-OH (where acyl = palmitoyl or stearoyl) were synthesized using standard fluoren-9-ylmethoxy carbonyl-based solid-phase chemistry with *t*-butyl and *S*-tritryl protecting groups for threonine and cysteine residues, respectively, and incorporating the fatty acyl residue in the final coupling cycle. After cleavage from the resin with 94/4/2 (v/v) trifluoroacetic acid/1,2-ethanedithiol/water, the crude acylpeptides were purified by flash chromatography on silica gel 60 with a gradient of 5–15% methanol in methylene chloride. The purified product was S-deprotected with 1,4-butanedithiol (Shahinian and Silvius, 1995), labeled with monobromobimane (Silvius and l'Heureux, 1994), purified by thin-layer chromatography on Whatman K6 silica gel 60 plates (Fisher Scientific, Ville St. Laurent, Québec), and developed with 88:12:0.2 methylene chloride/methanol/acetic acid. The bimane-labeled acylpeptides were reacted for 2 h at 25°C with 1.2 molar equivalents of α-amino-ω-methoxyPEGs or ethanolamine in dimethylformamide in the presence of benzotriazole-1-yl-oxy-tris-pyrrolidino-phosphonium hexafluorophosphate, *N*-hydroxybenzotriazole, and diisopropylethylamine (1.5, 1.5, and 3 molar equivalents, respectively). After the products were partitioned in 2:1:1 (v/v) methylene chloride/methanol/0.1 M aqueous HCOONa (pH 3.0), the lower layer was concentrated in vacuo, and the products were purified by thin-layer chromatography in 88:12:0.5 (for PEG350 and -750 conjugates) or 85:15:0.5 (for PEG2000 and -5000 conjugates) methylene chloride/methanol/acetic acid. The purified conjugates were stored as methylene chloride solutions at −20°C.

Conjugate/vesicle binding measurements

Lipid vesicles (9:1 egg PC/POPE containing additional lipid components as indicated) were prepared by mixing all lipids as stock solutions in chloroform, drying down first under nitrogen and then under high vacuum for several hours and hydrating at 25°C to 20–40 mM lipid in buffer (150 mM NaCl, 5 mM TES, 0.1 mM EDTA, pH 7.2, at 37°C). After vortexing, and freeze-thawing three times, the lipid suspension was hand-extruded through a 0.1-μm pore size polycarbonate filter (MacDonald et al., 1991). The average diameter of the extruded vesicles (9:1 egg PC/POPE) was determined to be 120 ± 2 nm by dynamic light scattering.

Vesicle stability was tested by measuring the rate of leakage of entrapped calcein (50 mM, in 20 mM NaCl, 5 mM TES, 0.1 mM EDTA, pH 7.2 at 37°C). After separation of vesicles from unencapsulated calcein solution on a Sephadex G-50 column, the spontaneous release of the dye was monitored by relief of self-quenching as described previously (Allen and Cleland, 1980), and 20 μl of Triton X-100 was added at the end of each run to determine the fluorescence intensity representing 100% dye release.

Lipid concentrations of vesicle suspensions were determined by sample digestion and phosphorus analysis (Lowry and Tinsley, 1974). The fraction of total vesicle lipids in the external leaflet was estimated from the fraction of surface-exposed POPE by the assay of Nordlund et al. (1981), with the modification that the time of incubation with the trinitrobenzenesulfonic acid reagent was shortened to 10 min. These data were combined to calculate the concentration of lipids exposed at the vesicles' outer surface (L_{eff}).

All binding measurements were carried out as described previously (Silvius and l'Heureux, 1994). Fluorescent acylpeptide-PEG conjugates were incorporated into the outer leaflet of preformed liposomes by injecting 4.5 nmol conjugate into 3 ml of a 0.1 mM vesicle suspension. The sample was incubated for 5 min at 37°C and then kept either at 0°C (ethanolamine, PEG350, and PEG750 conjugates) or at 25°C (PEG2000 or -5000 conjugates). Control experiments indicated that essentially 100% of the conjugate molecules in "carrier" vesicles prepared and maintained in this manner remained available for rapid transfer to subsequently added "acceptor" vesicles containing a fluorescence quencher, indicating that a negligible fraction of the conjugate molecules became trapped in the inner leaflet of the carrier vesicles.

Fluorescence measurements were carried out on a Perkin-Elmer LS-5 fluorimeter, using excitation and emission wavelengths of 390 nm and 468 nm, respectively (slits 15/20 nm). For each binding measurement, 0–800 nmol of unlabeled lipid vesicles was added to 2 ml buffer in the fluorimeter cuvette at 37°C with stirring. After the baseline signal was recorded, 10 nmol of the conjugate-containing "carrier" vesicle mixture was added. The resulting fluorescence change (a rapid rise followed by a slow decay due to conjugate adsorption to the cuvette) was recorded for a further 1–2 min and extrapolated to the moment of conjugate/carrier-vesicle addition. Fifteen to twenty data points collected in this manner were collected to provide each "binding curve," which was analyzed as described in Materials and Methods.

Estimates of conjugate fluorescence in the absence of any lipid (F_o) were obtained by injecting into the fluorimeter cuvette an amount of conjugate precisely matching that injected in the lipid-binding measurements carried out in the same experiment as just described. The conjugate fluorescence was measured before and after addition of unlabeled lipid vesicles at a concentration sufficient to give essentially 100% binding of the conjugate to lipid. The latter value was checked for consistency with the plateau fluorescence (at high lipid concentrations) estimated directly from the binding curve in the same experiment.

Possible micelle formation in mixtures containing PE-PEG5000 was examined by ^{1}H-NMR. Lipid suspensions (3.5–5 mM) containing 0–13 mol% PE-PEG5000 in egg PC/POPE (9:1 molar ratio) were prepared as above in 150 mM NaCl, 5 mM HEPES in 9:1 (v/v) D_2O/H_2O (pD = 7.3 at 37°C). Samples of pure PE-PEG5000 were prepared at lower concentrations (0.5–2 mM) to avoid viscosity-dependent broadening of the NMR peaks. ^{1}H-NMR spectra were recorded on a VXR-300 Varian spectrometer, using a 14-μs 60° pulse and a relaxation delay of 1.5 s between successive acquisitions, and saturating the water resonance (~4.7 ppm) before each acquisition. Each spectrum was obtained from 64 acquisitions. The area of the acyl-chain methylene peak in each spectrum was normalized first to the HEPES resonance at 3.85 ppm, which served as an internal intensity standard (Kenworthy et al., 1995b), and then to the lipid concentration. The resulting profile of normalized -CH_2- spectral intensity versus sample composition was used to estimate the percentage of micellar lipid present at each PE-PEG content as described in Results, assuming 0% and 100% micellar lipid in the samples containing 0 mol% or 100 mol% PE-PEG, respectively, and a linear variation of the normalized signal intensity with the proportion of micellar lipid present.

Monte Carlo simulations

MC simulations were used to examine the properties of a system of PEG chains end-grafted to a planar surface. The simulations were partly based on algorithms developed by Laradji et al. (1994) and Miao et al. (1996) for grafted polymer brushes, which were extended for application to systems with low grafting densities. The grafting points were randomly distributed in the surface (off-lattice), and the polymers were assumed to be fully flexible. The Edwards Hamiltonian (Doi and Edwards, 1986) was used to describe the total energy of the polymer layer. The Hamiltonian for a monodisperse system of **K** surface-grafted polymer chains, each composed

of $N + 1$ monomers, is written as follows:

$$\mathcal{H}\{r_i(n)\}/kT = 0.5 \sum_{i=1}^{K} \int_0^N dn(dr_i(n)/dn)^2 + V\{r_i(n)\} \quad (1)$$

where $r_i(n)$ represents the position of the nth monomer unit in the ith polymer and the monomer $n = 0$ of each chain is grafted to the surface. The first term on the right-hand side of Eq. 1 is the Gaussian stretching energy, i.e., the sum over the Gaussian stretches of two neighboring monomers on the same polymer chain. In the case of a good solvent the interaction potential between monomers, V, is approximated by the second term in the virial expansion of the interaction energy, which represents the excluded-volume interaction and which causes the polymer to swell. It is given by the expression

$$V\{r_i(n)\} = 0.5 w_2 \int dr \phi^2(r) \quad (2)$$

where w_2 (> 0) is the excluded-volume parameter for the case of a good solvent, and $\phi(r)$ is the local density of monomers:

$$\phi(r) = \sum_{i=1}^{K} \int_0^N dn \delta(r - r_i(n)) \quad (3)$$

The microscopic configurations of the grafted polymers are described by the spatial positions of the individual monomers. The basic constraint is that one end of the polymer chain is grafted randomly in the xy plane at $z = 0$, and all other monomers in each chain lie in the upper half-space ($z \geq 0$). To this we add the constraint that the grafting points cannot come closer than a distance **D**, representing the exclusion distance of two lipids in the membrane surface. With a mean estimated lipid area (a_L) of 64 Å^2 derived from the reported molecular areas of liquid-crystalline egg PC and POPE (Cevc, 1993) we obtained a value of 9 Å for the mean diameter of a lipid (D_{exp}). This distance is related to **D** by the equation $\mathbf{D} = D_{exp} \cdot \beta/b_{exp}$, where $\beta = \sqrt{3}$ is the dimensionless effective bond length between two monomers used in the MC simulations, and $b_{exp} = 3.5$ Å is the experimentally determined effective bond length (or Kuhn length) of PEG (Kenworthy et al., 1995a).

To calculate the energy for each configuration, the integrals in Eqs. 1 and 2 are replaced by sums. The Gaussian stretching term in Eq. 1 is thus determined as

$$0.5 \sum_{i=1}^{K} \sum_{n=0}^{N} [r_i(n) - r_i(n-1)]^2 \quad (4)$$

and the excluded volume interaction energy in Eq. 2 is calculated by dividing the system into a grid of cubic boxes of dimension β, counting the number of monomers in each box to find the local coarse-grained monomer density and summing the contributions from all boxes (Miao et al., 1996):

$$V\{r_i(n)\} = 0.5 w_2 \sum_{k=1}^{N_{box}} V_{box} \phi^2(k) \quad (5)$$

where N_{box} is the total number of boxes in the simulated system, $V_{box} = \beta^3$ is the volume of each box, and $\phi(k)$ is the monomer density (i.e., the number of monomers) in box k.

Simulations were carried out using the Metropolis MC method in real space, starting with an initial configuration of almost fully extended polymer chains with small fluctuations in the monomer positions. For each MC step the position of a randomly chosen monomer was altered, and the resulting energy change was computed using the Hamiltonian of Eq. 1 as just described, accepting or rejecting the change in position according to the energy change, using the Metropolis MC algorithm. For the PEG2000 system each simulation was performed with 10^6 MC steps per monomer, including equilibration of the system after 10^4 steps per monomer. For the PEG5000 system we performed 1.6×10^6 MC steps per monomer, including 8×10^5 steps, to reach the equilibrium. For both PEG systems average values were calculated from 4×10^4 MC steps at equilibrium.

PEG2000 and PEG5000 chains were calculated to have 57 and 143 effective bond lengths ($b_{exp} = 3.5$ Å) per polymer, using the expression $(M/M_{mono}) \cdot (b_{chem}/b_{exp})$, where M is the polymer molecular weight, the PEG monomer molecular weight M_{mono} is 44 g/mol, and $b_{chem} = 4.4$ Å is the length of a chemical monomer unit (Takahashi and Tadokoro, 1973). In the simulations the number of polymers grafted to the surface, **K**, was 80. The total surface area A_{tot} was varied to yield a range of grafting densities σ ($= \mathbf{K}/A_{tot}$) spanning the range of grafting densities s_{exp} ($= x_{PEG}/a_L$) examined in the conjugate-binding experiments described above. The relationship between σ and s_{exp} is given by the equation $\sigma = s_{exp} \cdot b_{exp}^2/\beta^2$, with $\beta = \sqrt{3}$.

The excluded volume parameter w_2 was set (somewhat arbitrarily) as 0.1 based on the only literature value available for PEG in an aqueous medium ($w_2 = 0.05$ for PEG in water at 27°C (Huggins, 1943; Brandrup and Immergut, 1966)) and taking account of the fact that our experiments were performed in an electrolyte medium at 37°C. The results of our simulations were not significantly affected when w_2 was decreased to 0.05.

The free accessible area (A_{acc}) available for binding of additional polymers at each grafting density of the simulated PEG2000 and PEG5000 polymers was determined by projecting the final configuration of the polymer layer onto the surface plane, which was subdivided into squares of length equal to the effective bond length. Each square in the projection plane was then scored as occupied if the x, y coordinates of a monomer fell into it and as "free" otherwise. Because of the periodic boundary condition, free squares on one side of the grafting area were considered to be connected with free squares on the opposite side. The number of squares occupied per grafted polymer (N_{poly}) was obtained by dividing the number of occupied squares by the number of grafted polymers, **K**. Clusters of contiguous free squares (defined as groups of free squares in which neighboring squares share an edge) were identified, the number of squares belonging to each such cluster (N_s) was determined, and the total number of accessible free squares N_{acc} was calculated as the sum of the N_s values over all clusters fulfilling the condition $N_s \geq N_{poly}$. In cases where we wished to estimate the accessible free area available for reversible binding of a "guest" (acylpeptide-PEG) polymer of a size different from that of the permanently grafted "host" (PE-PEG) polymers, we used for the "guest" polymer the value of N_{poly} estimated from a simulation where the grafted polymer chains were the size of this polymer. In this manner we obtained the value of N_{acc} appropriate to the dimensions of the "host" and "guest" polymer chains, as well as the total number of squares N_{tot} and the ratio $N_{acc}/N_{tot} = A_{acc}/A_{tot}$ for each mole fraction of PE-PEG simulated. The mean surface area occupied per polymer (N_{poly}) was likewise determined from the above square-counting algorithm.

RESULTS

Binding of acylpeptide-PEG conjugates to "bare" egg PC/POPE bilayers

In Fig. 1 is shown the general structure of the acylpeptide-PEG conjugates whose binding to lipid vesicles was examined in this study. The short peptide segment -GTC(bimanyl)G- in these conjugates served to provide a site of attachment for the fluorescent bimanyl group and to position this group slightly away from the acyl group, affording an optimal degree of fluorescence enhancement upon binding to the vesicle surface. Although we will describe these conjugates as "acylpeptide-PEGs" in this report, these conjugates are in essence acylated PEGs incorporating a small fluorescent-labeled spacer. As discussed below, measure-

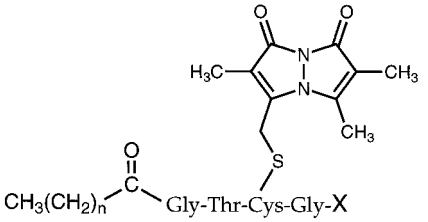

FIGURE 1 General structure of fluorescent acylpeptide-PEG conjugates, where the acyl group RCO- is a palmitoyl or stearoyl moiety and the residue -X is either an ethanolamine or an α-amino-ω-methoxy-PEG residue in amide linkage to the peptide linker carboxy-terminus.

ments of the reversible binding of low concentrations of these conjugates to lipid vesicles containing varying concentrations of PE-PEGs allowed us to "probe" the state of the grafted polymer layer as a function of the grafting density.

The affinity of binding of bimane-labeled acylpeptide-PEGs to lipid vesicles (with or without permanently surface-grafted PEG chains in the form of PE-PEGs) was determined by a fluorescence assay as described previously (Silvius and l'Heureux, 1994). Conjugate molecules, preincubated with a low concentration of "carrier" vesicles, were rapidly equilibrated with additional lipid (at varying concentrations) in the fluorimeter cuvette, and the relationship of the final fluorescence value to the lipid concentration was analyzed as described below to determine the affinity of conjugate binding to the vesicle surface.

As discussed previously (Peitzsch and McLaughlin, 1993; Silvius and l'Heureux, 1994), the distribution of acylpeptide-PEG conjugates between their aqueous (P_{aq}) and vesicle-bound (P_{ves}) forms is described by a dimensionless mole fraction-based partition coefficient K_p or, equivalently (at mM or lower lipid concentrations), by an effective dissociation constant $K_d^{eff} \equiv [P_{aq}] \cdot L_{eff}/[P_{ves}]$, where L_{eff} is the concentration of surface-exposed vesicle lipids to which the conjugate has ready access. If the fluorescence per unit mass of the aqueous and vesicle-bound forms of the conjugate differs, the fluorescence of a fixed amount of conjugate will vary with the lipid concentration according to the equation

$$F = F_o + (F_{max} - F_o) \cdot (L_{eff}/(K_d^{eff} + L_{eff})) \qquad (6)$$

where F_o is the fluorescence of the acylpeptide-PEG conjugate in the complete absence of lipids and F_{max} is the fluorescence when all conjugate molecules are bound to vesicles. In Fig. 2 we show the fit to Eq. 6 of a representative set of fluorescence data, obtained using a constant amount of palmitoyl-GTC(bimanyl)G-PEG750 in the presence of varying amounts of 9:1 (molar proportions) egg PC/POPE vesicles.

In Fig. 3 are summarized the values of K_d^{eff} measured for the association with "bare" lipid vesicles of palmitoylpeptide-PEG conjugates incorporating PEG residues of varying size. It can be seen that the binding affinity decreases

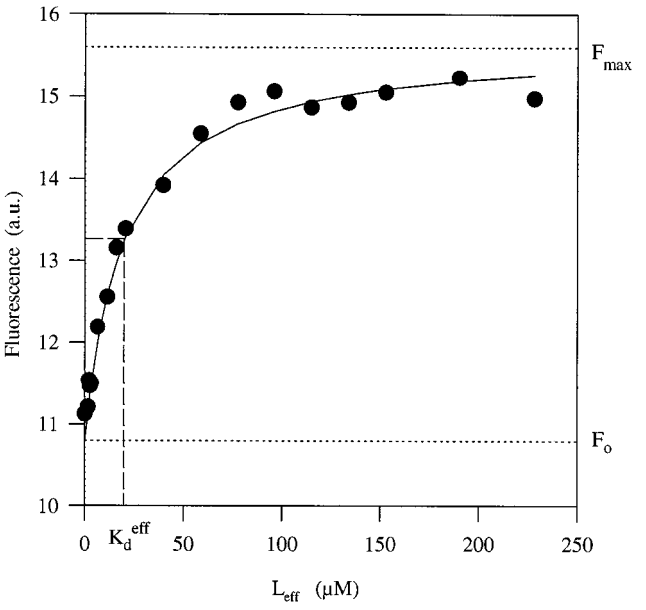

FIGURE 2 Representative binding curve, fit to Eq. 6, for association of stearoyl-GTC(bimanyl)G-PEG750 with large unilamellar 9:1 (molar proportions) egg PC/POPE vesicles. Details of the binding measurements and their analysis were as described in the text.

markedly as the size of the PEG-moiety increases, such that the value of K_d^{eff} measured for the PEG5000 conjugate is some 27-fold greater than that for the ethanolamine ("PEG monomer") conjugate. This result is consistent with predictions that the association of hydrophilic or amphiphilic

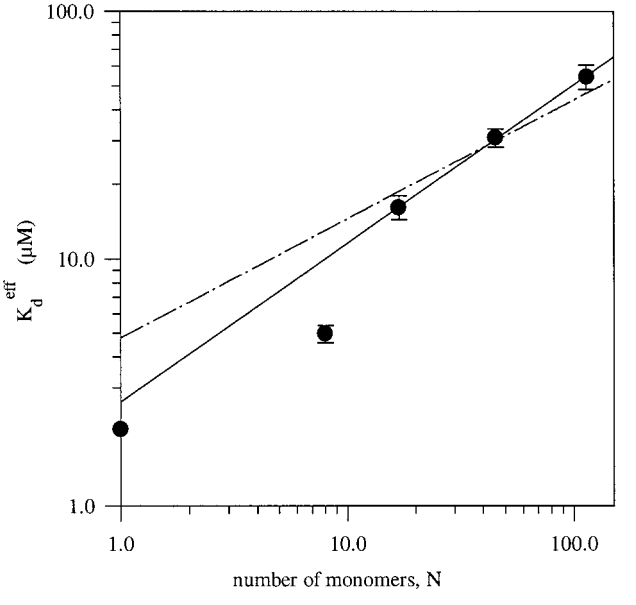

FIGURE 3 Effective dissociation constants K_d^{eff} for binding of different palmitoyl-GTC(bimanyl)G-ethanolamine or -PEG conjugates to large unilamellar 9:1 (molar proportions) egg PC/POPE vesicles. Each data point represents the mean ($\pm$ SD) of four to six independent experiments. ——, The best power-law fit to the data for PEG750, -2000, and -5000 conjugates (slope = 0.64); – · –, the theoretical relationship expected for very long polymer chains (slope = 0.48).

polymers with lipid bilayers can entail a significant (and size-dependent) loss of configurational, rotational, and/or translational entropy (Janin and Chothia, 1978; Finkelstein and Janin, 1989; Silvius and Zuckermann, 1993). The limiting slope for larger PEG conjugates in a double-logarithmic plot of K_d^{eff} versus the number of PEG monomers per chain (Fig. 3) is 0.64. As will be discussed later, this value is qualitatively consistent with but somewhat higher than the value of 0.48 predicted for very long polymers.

In the experiments summarized in Fig. 3 the level of acylpeptide-PEG conjugates present in the surface of the lipid vesicles was estimated under all conditions to be less than 0.2 mol% and usually much lower. As demonstrated in the next section, under these conditions interactions between PEG chains should have a negligible effect on the affinity of conjugate binding to lipid vesicles.

Binding of acylpeptide-PEG conjugates to PE-PEG-containing bilayers

In Fig. 4 we summarize the results of a series of measurements of the affinity of partitioning of stearoylpeptide-PEG2000 and -PEG5000 conjugates into lipid bilayers containing varying mole fractions of PE-PEG2000 or PE-PEG5000. For each experiment, K_d^{eff} was determined in parallel for the stearoylpeptide-PEG conjugates just noted and, as a reference, for the analogous palmitoylpeptide-ethanolamine conjugate. The values of K_d^{eff} measured for the stearoylpeptide-PEG conjugates were then normalized to the value measured for the palmitoylpeptide-ethanolamine conjugate (using the same vesicle preparation for all three compounds). Determination of this ratio of dissociation constants ($\mathcal{H}_d$) served to minimize possible effects of batch-to-batch variation in vesicle preparations and, more fundamentally, to factor out possible variations in the free energy of binding of the acylated peptide moiety itself to bilayers of different PE-PEG contents. In practice, however, this latter variation was found to be small (not shown).

It is evident from the results shown in Fig. 4 that the affinity of binding of acylpeptide-PEG conjugates to lipid surfaces can be greatly diminished by the presence of permanently grafted PEG chains (PE-PEGs) at grafting densities typical of those used to prepare "sterically stabilized" lipid vesicles. This is particularly evident for the binding of acylpeptide-PEG5000 conjugates to vesicles containing PE-PEG5000, where the presence of 6 mol% of the latter species reduces the affinity of binding of the former by 16-fold, corresponding to a reduction in the free energy of binding of 1.71 kcal mol^{-1} (Fig. 4 *D*). Significantly, in the range of PE-PEG2000 and PE-PEG5000 contents examined, the data of Fig. 4 reveal no evident discontinuity such as might be expected if the polymer chains exhibited a sharp conformational transition with increasing chain grafting density. As described later, this dramatic variation in conjugate binding affinity with the grafting density of PEG chains can be satisfactorily accounted for on the basis of our simulations of the configurations of the grafted polymer chains and their effects on the accessible free area exposed at the vesicle surface.

To confirm that the results shown in Fig. 4 were not significantly affected by the negative charge of the PE-PEGs (Woodle et al., 1992), we also examined the binding of the ethanolamine, -PEG2000, and -PEG5000 conjugates to egg PC/POPE vesicles incorporating varying mole fractions of POPG in place of PE-PEGs. In these experiments (not shown) we found that variation of the vesicle POPG content from 0 to 10 mol% had no significant influence on the measured vesicle-binding affinity of the conjugates.

Vesicle stability and PE-PEG-induced micelle formation

To ensure that the data described above were amenable to modeling by the simulations discussed in the next section, it was important to establish that the lipid dispersions examined adopt a bilayer organization with minimal content of micellar structures, which can form in dispersions containing high levels of PE-PEGs (Lasic et al., 1991b; Woodle and Lasic, 1992; Hristova and Needham, 1995; Kenworthy et al., 1995b; Bedu-Addo et al., 1996). For PC/PE-PEG2000 mixtures, micellar structures have been observed only above 15 mol% PE-PEG (Hristova et al., 1995; Hristova and Needham, 1994), outside the range of PE-PEG2000 contents examined here. However, as a recent report (Baekmark et al., 1997) has suggested that mixtures containing much lower levels of PE-PEG5000 may contain micellar structures, we used ^{1}H-NMR measurements to test directly the possible existence of micelles in egg PC/POPE/PE-PEG5000 mixtures of varying PE-PEG content. The method was based on the change in the peak area of the lipid acyl-chain methylene resonance as a function of lipid aggregate structure (Finer et al., 1972). A relatively sharp peak is observed for micelles, whose tumbling is sufficiently rapid on the NMR time scale to average out dipolar couplings. By contrast, under the NMR conditions used here, the much broader acyl-chain -CH_2- peak arising from lipids in large unilamellar vesicles is poorly resolved from the baseline. As a result, a given quantity of phospholipid will give a much larger integrated intensity for the acyl-chain methylene resonance when the lipids exist in micellar form than when the lipids are present in large vesicles. As shown in Fig. 5, the integrated acyl-chain methylene peak intensity for dispersions containing varying levels of PE-PEG5000 in 9:1 (molar proportions) egg PC/POPE is essentially constant from 0 to 6 mol% PE-PEG5000, indicating that only vesicles are present in this range of compositions. However, the integrated intensity begins to increase, indicating the appearance of a population of micellar structures, as the PE-PEG5000 content increases to 8 mol%. This result is in reasonable agreement with previous findings for sphingomyelin/egg PC/PE-PEG5000 mixtures (Allen et al., 1991). Accordingly, the analysis of the conjugate-binding data

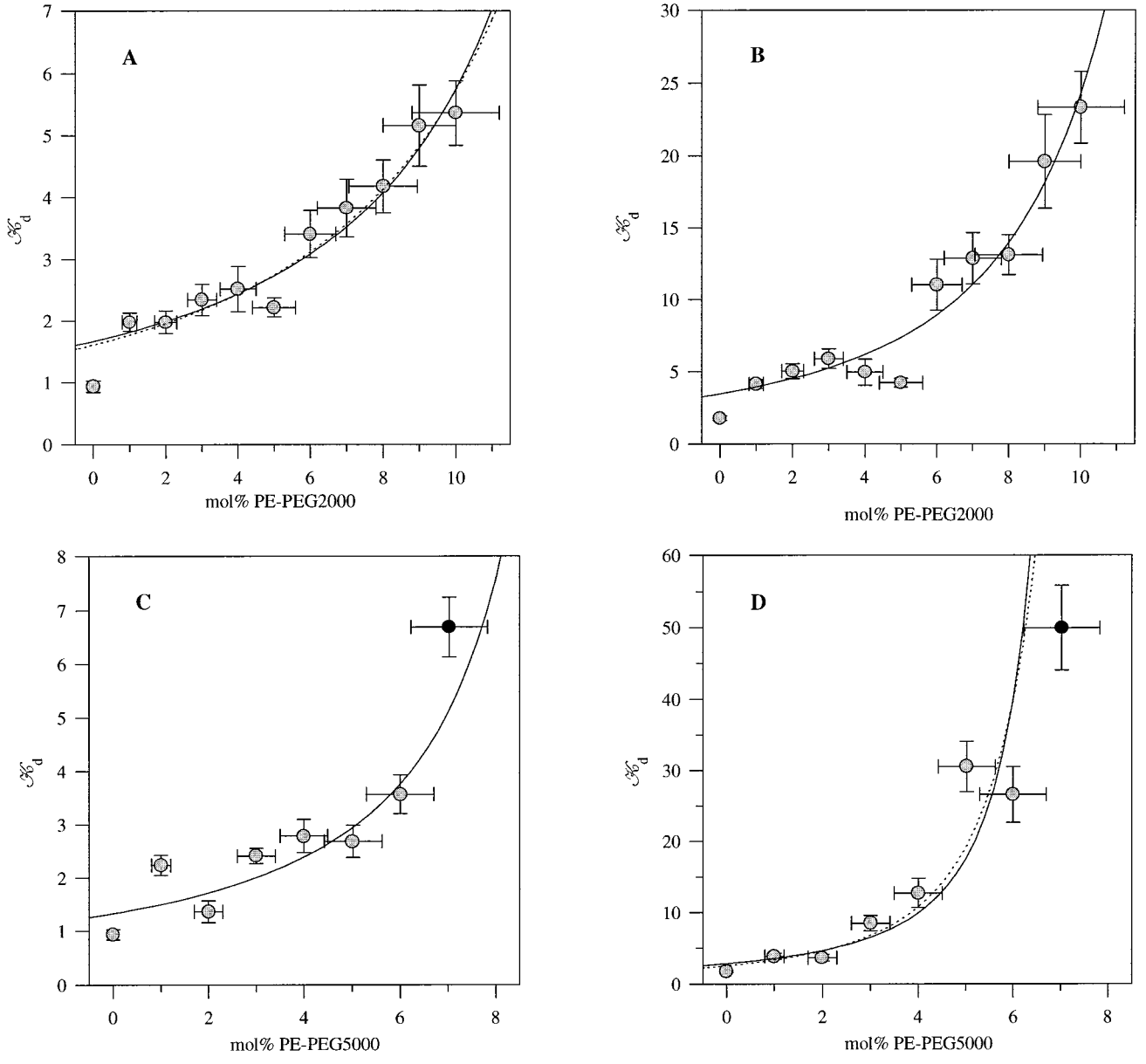

FIGURE 4 "Normalized" dissociation constants $\mathcal{K}_d$, determined as described in the text, for binding of stearoylpeptide-PEG2000 or -PEG5000 conjugates to large unilamellar egg PC/POPE vesicles containing PE-PEGs. (*A* and *B*) Binding of acylpeptide-PEG2000 (*A*) or -PEG5000 (*B*) to vesicles containing the indicated molar percentage of PE-PEG2000. (*C* and *D*) Binding of acylpeptide-PEG2000 (*C*) or -PEG5000 (*D*) to vesicles containing the indicated molar percentage of PE-PEG5000. ——, The best fits of Eq. 9 (*A* and *D*) or Eq. 11 (*B* and *C*) to the data modeling the surface-grafted polymer chains as a van der Waals gas; ····· (*A* and *D*), the best fits of Eq. 10 to the data modeling the grafted chains as a set of hard discs. Data shown represent the mean (± SD) of two to four independent experiments for each vesicle composition. The data for 7 mol% PE-PEG5000 in *B* and *C* were omitted from the fit because of the possible presence of micelles at this level of PE-PEG.

shown in Fig. 4 in the light of simulations described later was confined to samples containing 0–10 mol% PE-PEG2000 or 0–6 mol% PE-PEG5000.

In further experiments to assess the possible effects of PE-PEGs on vesicle stability, we examined the release of calcein from vesicles incorporating 10 mol% PE-PEG2000 or 8 mol% PE-PEG5000, as described in Materials and Methods. No significant enhancement of the rate of calcein leakage or reduction in the level of trapped calcein was observed for vesicles of either of these compositions when compared to vesicles containing no PE-PEG, supporting our conclusion that the integrity of the vesicles used in our conjugate binding experiments was not compromised by the presence of the PE-PEGs. Edwards et al. (1997) have reported the presence of open as well as sealed bilayer structures in lipid mixtures containing more than ~10 mol% PE-PEG2000. These calcein-trapping results, and our finding using the assay of Nordlund et al. (1981) that <60% of vesicle PE was exposed to the extravesicular medium for all vesicle compositions (not shown), indicate, however, that

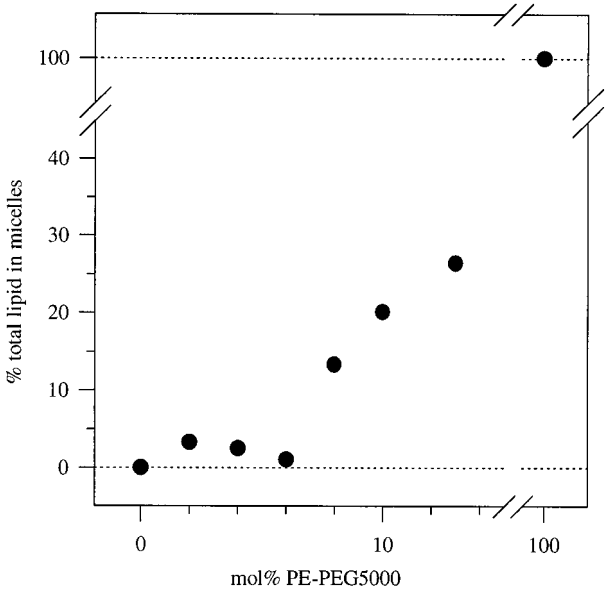

FIGURE 5 Percentage of total lipids present in micelles (determined by ^{1}H-NMR measurements as described in the text) as a function of PE-PEG content for egg PC/POPE (9:1 molar proportions) mixtures containing the indicated molar percentages of PE-PEG5000.

open bilayer structures must be at most a minor component of the lipid mixtures examined in this study.

Monte Carlo simulations

Alexander (1977) and de Gennes (1980, 1987) classify the state of a system of grafted polymers in a good solvent in terms of two regimes: a "mushroom" regime at low grafting density and a "brush" regime at high grafting density. In the mushroom regime the grafted polymers are relatively far apart, such that their conformations are only slightly affected by steric interactions with other chains. With increasing grafting density, steric interactions between neighboring polymers become progressively more significant, ultimately forcing the polymers to adopt a more extended brush configuration. For very long polymer chains a sharp (though not truly discontinuous) mushroom-brush transition has been predicted (de Gennes, 1980). In contrast, the experimental results discussed above suggest no abrupt discontinuity in the free energy of surface-associated medium-length PEG chains as the grafting density increases over the range examined.

To explore this behavior further and to obtain more information about characteristic properties of a grafted PEG2000 or PEG5000 layer, we carried out MC simulations of a planar surface bearing end-grafted PEG chains at different surface densities, as described in Materials and Methods. The simulations were performed for the same range of grafting density and for the same polymer lengths as were examined in the experiments described above. Hence the simulated systems represent the PE-PEG-containing surfaces that were "probed" by acylpeptide-PEG conjugates in the above binding experiments.

In Fig. 6 are shown snapshots (top view) of simulated PEG-lipid-containing membranes at various PEG-lipid densities as calculated by the Metropolis MC method. For simulated surfaces containing 2 mol% PEG2000- and PEG5000-lipids (Fig. 6, *A* and *C*, respectively), a large amount of free area remains on the surface, whereas the simulated surfaces containing 10 mol% PEG2000-lipids (Fig. 6 *B*) or 6 mol% PEG5000-lipids (Fig. 6 *D*) exhibit much less free area, as expected. It can be seen that the surface containing 6 mol% PEG5000-lipids exhibits markedly less free area than that containing 10 mol% PEG2000-lipids.

In Fig. 7 *A* we show density profiles $\phi(z)$ of the polymer layer in the z direction (normal to the grafting surface) for simulated surfaces bearing various mole fractions (x_{PEG}) of PEG2000 (*open symbols*) or PEG5000 chains (*closed symbols*). In this figure $\phi(z)$ gives the density of monomers at a distance z above the surface. In the experimental range of x_{PEG} the density profiles $\phi(z)$ for membranes containing either type of grafted chain change only slightly with x_{PEG}.

Fig. 7 *B* gives the averaged profile of the radius of gyration in the xy plane as a function of distance from the surface, $R_{Gx,y}(z)$, for end-grafted PEG chains at a surface coverage corresponding to 6 mol% PE-PEG2000 (*open symbols*) or PE-PEG5000 (*filled symbols*). Comparison of the profiles demonstrates, as expected, that with increasing PEG chain length the function $R_{Gx,y}(z)$ reaches a higher maximum value and peaks at a larger value of z. The radius-of-gyration profiles showed no significant variation with the density of grafted PEG over the range equivalent to 0–10 mol% PE-PEG2000 and 0–6 mol% PE-PEG5000 (not shown). Comparison of the radii of gyration of grafted PEG chains in the xy plane to those along the z axis indicated that the polymer chains were relatively extended, even at low polymer grafting densities, with an rms extension along the z axis some four- to fivefold greater than that in the xy plane.

Calculations of the average internal energy for surface-grafted PEG2000 or PEG5000 chains showed no significant variation in the range of grafting densities examined experimentally (not shown). The finding that the density profiles, the profiles of the radius of gyration $R_{Gx,y}(z)$, and the average internal energy per polymer for both types of grafted PEG systems do not vary substantially with grafting density in our simulations (again, over the range of grafting densities examined experimentally) indicates that the PEG2000- and PEG5000-grafted surfaces remain in the mushroom regime throughout the range 0–10 mol% PE-PEG2000 and 0–6 mol% PE-PEG5000.

Calculation of the accessible free area

The above simulations suggest that the surface-associated PEG chains exhibit little change in mean conformation as

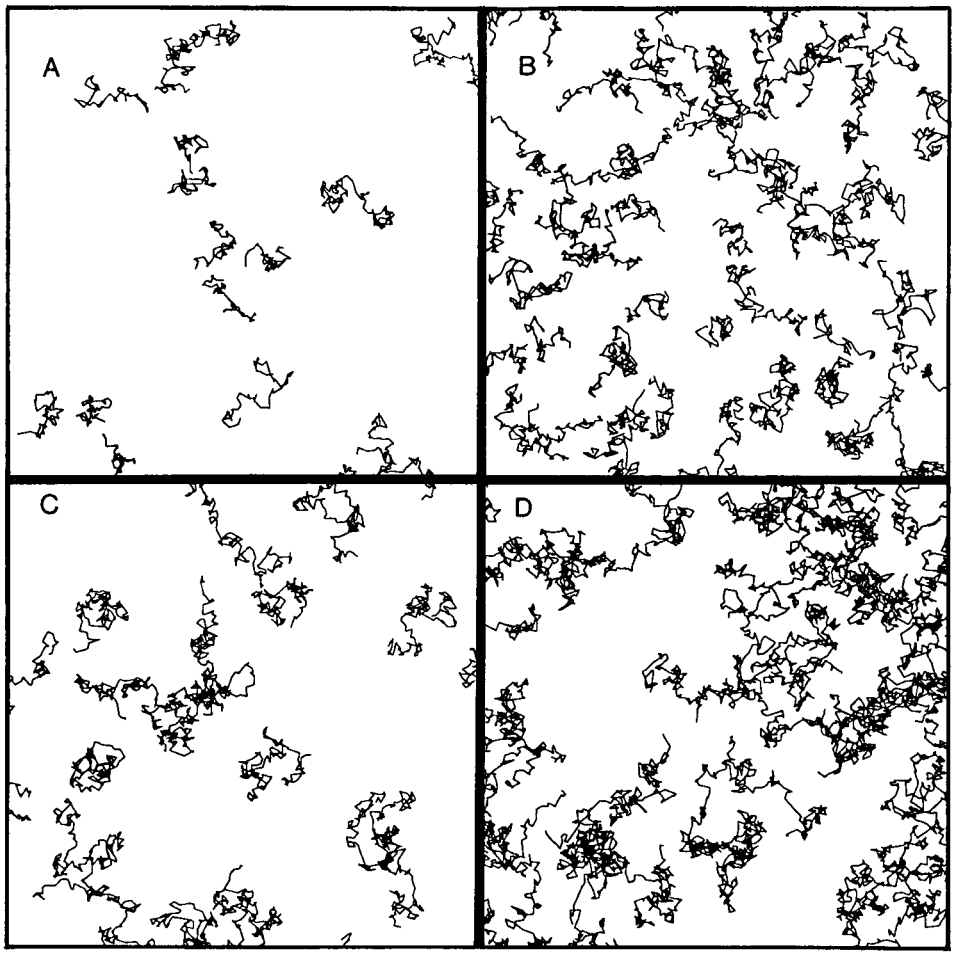

FIGURE 6 "Snapshot" (top) views of MC-simulated lipid surfaces containing PEG-lipids. (*A* and *B*) Simulated surfaces containing 2 mol% (*A*) or 10 mol% (*B*) PEG2000-lipid. (*C* and *D*) Simulated surfaces containing 2 mol% (*C*) or 6 mol% (*D*) PEG5000-lipid. Each panel represents a surface area equal to that of the others.

the PEG grafting density is varied within the range examined experimentally. It thus appears that the markedly weaker binding of acylpeptide-PEG conjugates to PE-PEG-containing as opposed to "bare" lipid membranes (Fig. 4) cannot be ascribed to a greater reduction in the configurational entropy of an acylpeptide-PEG polymer chain when the conjugate binds to a surface containing higher levels of PE-PEG. This consideration suggests, in turn, that a decrease in accessible free area (i.e., the area accessible for binding of additional polymer molecules) could be the major determinant of the diminished affinity of binding of acylated PEGs to lipid surfaces already containing permanently grafted (PE-PEG) polymer chains. Accordingly, we used the above simulations to evaluate the proportion of accessible free area as a function of the density of grafted (PE-) PEG chains.

We applied a square-counting algorithm to all snapshots obtained from our MC simulations (examples of which are shown in Fig. 6) to calculate the proportion of accessible free area (A_{acc}/A_{tot}) as a function of the mole fraction of PEG-lipids, x_{PEG} (see Materials and Methods). As shown in Fig. 8, the dependence of the ratio (A_{acc}/A_{tot}) on x_{PEG} up to 10 mol% PEG2000- or 6 mol% PEG5000-lipid can be described by a linear function:

$$A_{acc}/A_{tot} = 1 - Bx_{PEG} \quad (7)$$

where the dimensionless parameter B represents the ratio of the average surface area covered by a single PEG chain to the mean area per lipid. The values of B obtained from the MC simulations for each combination of acylpeptide-PEG conjugate and PE-PEG examined experimentally are given in Table 1.

Comparison of simulation and experimental results

The variation of the normalized K_d^{eff} values ($\mathcal{H}_d$) for binding of a given acylpeptide-PEG conjugate to bilayers containing varying mole fractions (x_{PEG}) of a given PE-PEG (Fig. 4) can be described by the following general equation:

$$\mathcal{H}_d(x_{PEG}) = \mathcal{H}_d^o \cdot f(x_{PEG}) \quad (8)$$

where $\mathcal{H}_d^o$ is the value of $\mathcal{H}_d$ when $x_{PEG} = 0$, and the function $f(x_{PEG})$ takes the forms described below for different models of the behavior of the grafted polymers. In the following we distinguish between two cases where the dissociable "guest" polymer (acylpeptide-PEG) and the permanently grafted "host" polymer (PE-PEG) carry PEG chains of the same size (case I) or of different sizes (case II). We have considered the "guest" and "host" PEG-polymers situated on the membrane surface either as a van der Waals

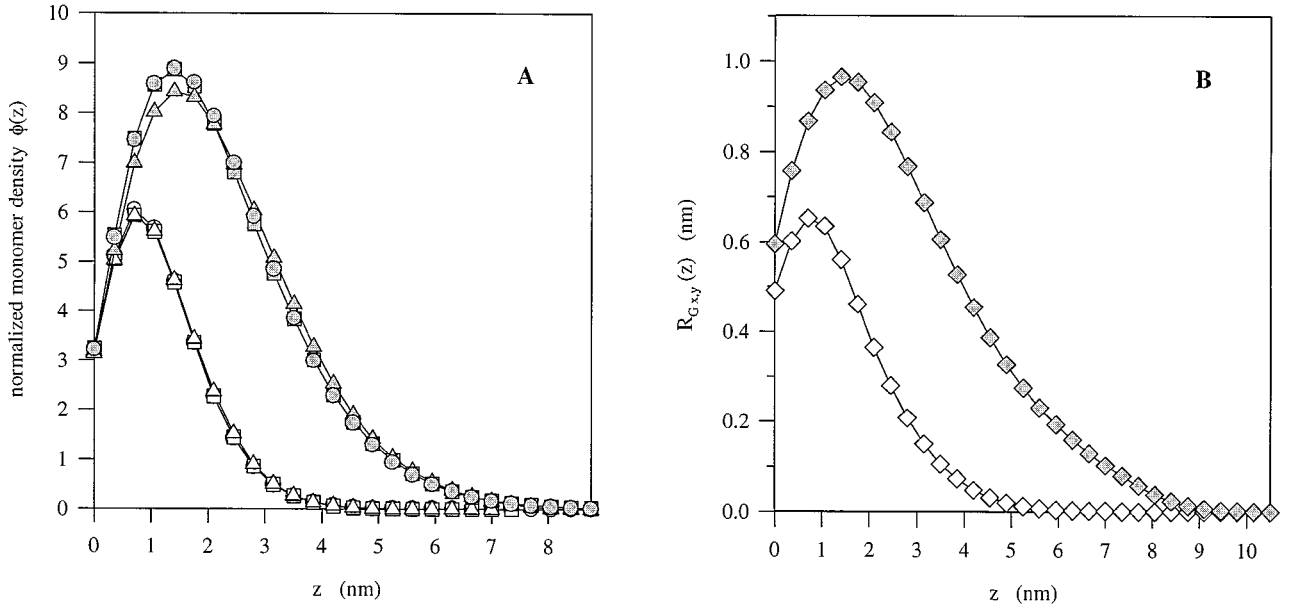

FIGURE 7 (*A*) Monomer density profiles $\phi(z)$ (normal to the grafting surface), normalized to the grafting density σ, from MC simulations of PEG-lipid-containing lipid surfaces at varying grafting densities. The simulated surfaces contained PEG chains at grafting densities equivalent to 2, 6, or 10 mol% PE-PEG2000 (white circles, triangles, or squares, respectively) or to 2, 4, or 6 mol% PE-PEG5000 (gray circles, triangles, or squares, respectively) in a fluid lipid bilayer. (*B*) Profiles of the radius of gyration in the *xy* plane, $R_{Gx,y}(z)$, from MC simulations of grafted PEG2000 (*white symbols*) or PEG5000 (*gray symbols*) chains at a surface density equivalent to 6 mol% PE-PEG in a fluid lipid bilayer. Note that the extension of the chains is significantly larger in the *z* direction than in the *xy* plane.

gas with negligible attractive interactions or as hard discs according to scaled particle theory (Helfand et al., 1961; Henderson, 1975). The thermodynamically based derivations of the appropriate forms of the function $f(x_{PEG})$ are given in the Appendix.

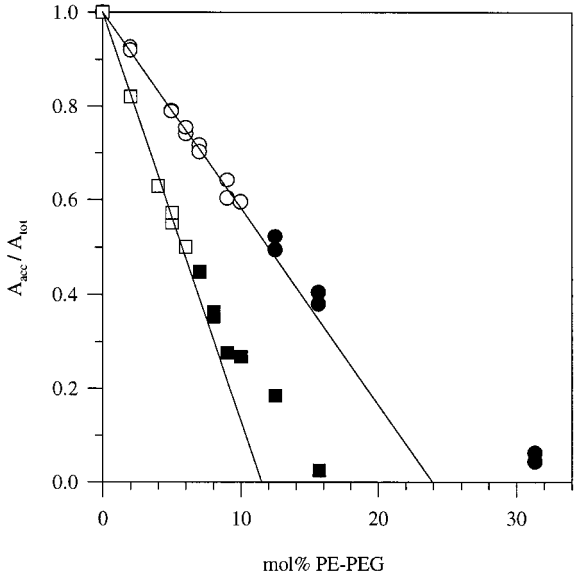

FIGURE 8 Fraction of accessible free area (A_{acc}/A_{tot}) calculated from MC simulations as a function of the molar percentage of PE-PEG2000 (*circles*) or -PEG5000 (*squares*). Open symbols represent data obtained for grafting densities corresponding to the experimental range of PE-PEG contents, which are well described by linear functions, as shown.

Case I

If we assume that a system of grafted "host" and "guest" PEG-moieties of equal size behaves like a van der Waals gas with negligible attractive interactions, we predict the relation

$$\mathcal{H}_d = \mathcal{H}_d^o \cdot w \cdot \exp(w - 1) \tag{9}$$

whereas if the PEG chains behave as a set of rigid discs, scaled particle theory leads to the relation

$$\mathcal{H}_d = \mathcal{H}_d^o \cdot w^{7/8} \cdot \exp((9w^2 + 7w - 16)/8) \tag{10}$$

(see Appendix), where $w = A_{tot}/A_{acc}$ can be described by the function $w = 1/(1 - B \cdot x_{PEG})$ in the range of PE-PEG concentrations examined experimentally (see Fig. 8). As noted above, the parameter B is the ratio of the average surface area occupied by a PEG chain to the mean surface area per lipid. The conjugate-binding data of Fig. 4, *A* and *D*, were fitted using either of the above equations with $\mathcal{H}_d^o$ and B as adjustable parameters, and the values of B thereby determined are listed in Table 1 along with the values of this parameter calculated from our MC simulations. For the binding of the acylpeptide-PEG2000 conjugate to bilayers containing PE-PEG2000, fitting the data to Eq. 9 yields an estimate of B very close to that calculated from the MC simulations, whereas fitting the data to Eq. 10 yields a substantially higher B value, suggesting that the surface-grafted PEG chains behave more like a van der Waals gas than as a set of rigid discs. (The values of B estimated from our MC simulations were not strongly dependent on the

TABLE 1 Values of the parameter *B* determined from MC simulations or by fitting the data of Fig. 4 to Eqs. 9 or 11 (van der Waals gas model) or Eq. 10 (hard-disc model)

		B value estimated from		
PE-PEG chain	Acylpeptide-PEG chain	MC simulations	Data fitting (van der Waals)*	Data fitting (hard disc)#
PEG2000	PEG2000	4.14 ± 0.04	4.1 ± 0.2	2.3 ± 0.1
	PEG5000	4.14 ± 0.03	4.1 ± 0.2	ND§
PEG5000	PEG2000	8.7 ± 0.2	10.4 ± 0.8	6.3 ± 0.5
	PEG5000	8.6 ± 0.1	7.7 ± 1.5	ND

**B* values listed in this column were estimated by fitting the experimental data to Eq. 9 (first and last entries in column) or Eq. 11 (second and third entries in column).

#*B* values listed in this column were estimated by fitting the experimental data to Eq. 10.

§ND, Not determined.

value chosen for the parameter w_2. Thus, for example, for the case of an acylpeptide-PEG5000 conjugate binding to a surface containing PE-PEG5000, we estimated *B* values of 8.7 and 9.6, respectively, from simulations assuming values of 0.1 and 1.0 for w_2.) The estimated value of *B* suggests that at low grafting densities a single PEG2000 chain occupies a surface area equivalent to roughly four lipid molecules (~2.6 nm^2 based on the *B* values estimated either from the MC simulations or by fitting the data of Fig. 4 *A* to Eq. 9). For binding of acylpeptide-PEG5000 to vesicles containing PE-PEG5000, Eqs. 9 and 10 yield estimated *B* values bracketing the value calculated from the MC simulations, suggesting that the behavior of the grafted PEG5000 chains is intermediate between that of a van der Waals gas and that of a set of rigid discs. The value estimated for *B* in this case suggests that at low grafting densities a PEG5000 chain occupies a surface area equivalent to approximately nine lipids (5.6 nm^2 from the simulations or 4.0–6.7 nm^2 from fitting the data of Fig. 4 *D* to Eqs. 9 or 10).

Case II

Describing a system of grafted "guest" and "host" polymer chains of different sizes as a van der Waals gas with negligible attractive interactions gives the following equation, which is a generalized form of Eq. 9 (see Appendix):

$$\mathcal{H}_d = \mathcal{H}_d^o \cdot w \cdot \exp(R \cdot (w - 1)) \qquad (11)$$

where $\mathcal{H}_d^o$ and *w* are defined as above, and $R = a_G/a_H$ is the ratio of the average cross-sectional areas of the reversibly bound "guest" polymer (acylpeptide-PEG) and the permanently bound "host" polymer (PE-PEG). An analogous derivation using scaled particle theory was not attempted, because the equation of state used in this approach cannot be applied to a mixture of discs of different sizes. To fit the experimental data in Fig. 4, *A–D*, with only two adjustable parameters, we estimated the value of *R* in Eq. 11 from our MC simulations, which gave average areas per PEG-polymer of 2.57 nm^2 and 5.27 nm^2, respectively, for bilayer-tethered PEG2000 and PEG5000 chains over the range of grafting densities examined experimentally. (The polymer area estimates noted here are calculated in a manner somewhat different from the calculations of those based on the *B* estimates described earlier in this section (specifically, they are determined for a particular polymer chain rather than for a particular pair of "host" and "guest" chains) and are consequently slightly different from the area estimates determined from the *B* values discussed above.) Similar values for the area of each type of polymer chain were estimated using profiles of the radius of gyration in the *xy* plane, $R_{Gx,y}(z)$ (not shown). Fitting the data of Fig. 4, *B* and *C*, and using Eq. 11 and the *R* values estimated as just described, we obtained the estimates of the parameter *B* listed in Table 1. In both cases the value of *B* estimated by fitting the data agrees well with that estimated from the MC simulations, also listed in Table 1.

In conclusion, the results obtained from our MC simulations are consistent with our experimental results for the reversible binding of small amounts of acylated PEGs to bilayers containing varying amounts of PE-PEGs.

DISCUSSION

Binding of acylpeptide-PEG conjugates to a "bare" lipid surface

The binding of acylpeptide-PEG conjugates of increasing PEG chain length to egg PC/POPE bilayers is expected to entail a certain loss of translational, rotational, and, especially, configurational entropy (Janin and Chothia, 1978; Finkelstein and Janin, 1989; Silvius and Zuckermann, 1993). For very long polymers in solution or grafted to a surface, the polymer chain partition functions are expected to scale as $Z_N = N^{\gamma - 1}$ and as $Z_{No} = N^{\gamma o - 1}$, respectively, where *N* is the number of monomers per chain and the exponents γ and γ_o have the values 1.16 and 0.68, respectively, in three dimensions (De'Bell and Lookman, 1993; Everaers et al., 1995). This leads to the prediction that the free energy of binding of acylpeptide-PEG conjugates to a "bare" planar lipid surface would vary with the PEG chain length according to the relation

$$\Delta G_p \propto 0.48 \cdot \ln N \qquad (12)$$

Fitting the data of Fig. 3 to the above equation, using only the data points for the higher molecular weight conjugates

(PEG750, -2000, and -5000) in light of the findings of Sarmoria and Blankschtein (1992), yields an estimated slope of 0.64, in qualitative agreement with but somewhat greater than the theoretical value of 0.48. This discrepancy may indicate that the polymers examined here are not well approximated as the very long polymer chains for which Eq. 12 was derived (Grosberg and Khokhlov, 1994; Götter et al., 1996; Szleifer, 1996).

Properties of surface-grafted PEG chains

The average energy of a grafted PEG2000 or PEG5000 chain calculated from our MC simulations corresponds to the average internal energy of the polymer and does not appear to vary significantly up to at least 10 mol% PEG2000-lipids or 6 mol% PEG5000-lipids. The relative constancy of the calculated chain density profiles (Fig. 7 *A*) and of the profiles of the radius of gyration $R_{Gx,y}(z)$ (not shown) with increasing x_{PEG} suggest no significant perturbation of the average configuration of the grafted PEG chains with increasing grafting density in this range of compositions. The attractive interactions between single grafted polymers are weak, and as our MC simulations indicate, the polymer chains are in a relatively extended configuration, even at low grafting densities (Fig. 7 *B*), such that no loss of configurational entropy of an individual grafted polymer is found as the density of grafted PEG chains increases (again, within the range of compositions noted above). As noted earlier, these results suggest that the decreased affinity of binding of acylpeptide-PEG conjugates to bilayers containing PE-PEGs cannot be explained by a greater loss of configurational entropy of the conjugate PEG chain upon binding to bilayers bearing grafted PEG chains. Instead, as discussed below, the decrease in accessible free area due to the presence of PE-PEGs appears to be the major factor underlying the markedly diminished affinity of the acylpeptide-PEG conjugates for PE-PEG-containing versus "bare" lipid surfaces.

The average cross-sectional areas in the *xy* plane determined from our MC simulations for grafted PEG2000 (2.57 nm^2) and PEG5000 chains (5.27 nm^2) agree well with the estimates obtained by fitting our experimental data. In the Alexander–de Gennes theory (Alexander, 1977; de Gennes, 1980, 1987, 1988) the area of a grafted polymer is calculated from the Flory radius R_F of the free polymer, which, in turn, is calculated as $R_F = b_{exp} \cdot N^{3/5}$ (Flory and Fisk, 1966), where b_{exp} is the effective bond length and N is the number of monomers. The Flory radius can be interpreted as the end-to-end distance of a polymer (Szleifer, 1996), in which case it can be taken as an effective diameter, giving an effective cross-sectional area $A_F = \pi {R_F}^2/4$. With $b_{exp} =$ 0.35 nm, we would thereby estimate cross-sectional areas of 12.3 nm^2 and 37.1 nm^2, respectively, for grafted PEG2000 and PEG5000 chains. (Not all workers interpret the Flory radius as an effective diameter, as is done here. However, if we consider the Flory radius to approximate the molecular radius, we would predict areas for the grafted PEG chains that are even larger, and hence even more divergent from our experimental and MC simulation estimates, than the values we estimate in the text.) These values are, respectively, 4.8- and 7.0-fold greater than the mean molecular areas calculated from our MC simulations. It is evident that a medium-sized grafted PEG chain is poorly described as effectively spherical. As illustrated in Fig. 7 *B*, the PEG moiety occurs instead in a relatively elongated conformation, even for the lowest PEG-lipid concentrations examined here.

Most published estimates of the area of a grafted PEG polymer are based on the Alexander–de Gennes theory, with the assumption that the Flory radius provides a reasonable estimate of the dimensions of the grafted polymer chain (Kuhl et al., 1994; Kenworthy et al., 1995a; Needham et al., 1997), and hence have yielded higher estimates than those reported here for the cross-sectional areas of a grafted PEG chain. From force-distance measurements, Kuhl et al. (1994) estimated the area of a grafted PEG2000 chain projected onto the bilayer surface to be ~9.6 nm^2 and ~4.8 nm^2, respectively, at 4.5 mol% and at 9 mol% PE-PEG2000, whereas we estimate a significantly smaller area (2.57 nm^2) that is moreover independent of the grafting density in this range. Evans and Rawicz (1997) suggested that at 10 mol% PE-PEG2000 or -PEG5000 lipids, the area per grafted PEG chain may be as small as ~7 nm^2, a value relatively close to our estimates for PE-PEG5000 but significantly higher than what we estimate for PE-PEG2000.

The Alexander–de Gennes theory predicts a sharp (though continuous) transition between mushroom and brush configurations of the tethered polymer chains. In this theory, in the mushroom regime ($D_{AdG} > R_F$, where D_{AdG} is the mean distance between grafting points) the extension length of the grafted layer is calculated as $L = R_F = b_{exp}N^{3/5}$, whereas in a brush regime ($D_{AdG} < R_F$) $L = Nb_{exp}^{5/3}D_{AdG}^{-2/3}$ (de Gennes, 1987, 1988). Using these equations for L, we would predict from Alexander–de Gennes theory that surface-grafted PEG chains (here, PE-PEGs) would undergo a mushroom-brush transition at a critical mole fraction of PE-PEG, given by

$$x_{PEG}^{crit} = 4a_L/(\pi b_{exp}^2 \cdot N^{6/5}) = 4a_L \cdot M_{mono}^{6/5}/(\pi b_{exp}^{4/5} \cdot M^{6/5} \cdot b_{chem}^{6/5}) \quad (13)$$

where M and M_{mono} (= 44 g/mol) are the molecular weight of the polymer and the monomer, respectively, and $a_L = 64$ $Å^2$ is the mean area per lipid. For bilayers containing grafted PEG2000 or PEG5000 chains in a solvent with $w_2 = 0.1$, a mushroom-brush transition is thereby predicted to occur at 6.8 mol% PE-PEG2000 or at 2.3 mol% PE-PEG5000, respectively. However, as the PEG-conjugate binding data shown in Fig. 4 do not indicate any abrupt transition with increasing bilayer PE-PEG content, we conclude that bilayers containing PE-PEGs either exhibit a gradual mushroom-brush transition or remain within the mushroom regime throughout the range of PEG grafting densities examined

experimentally. The results of our MC simulations favor the latter hypothesis. Besides the constancy of various characteristic parameters of the polymer layer (such as average chain energy, density profiles, and radius-of-gyration profiles) in the experimental range of PEG-lipid contents, our simulations also indicate that accessible free area still exists on the lipid surface, even for the highest grafting densities of PEG chains examined experimentally. We suggest that the deviation of our results from the predictions of Alexander–de Gennes theory indicates that PEG2000 and -5000 chains do not constitute sufficiently long polymers to fulfill the conditions of the Alexander–de Gennes model.

Our conclusion that lipid bilayers containing grafted PEG2000 chains (PE-PEGs) at densities up to 10 mol% remain in the mushroom regime is at variance with reports in the literature that systems containing 9 mol% PE-PEG2000 exist in a brush regime (Kuhl et al., 1994; Sheth and Leckband, 1997; Majewski et al., 1997). Szleifer (1996) has concluded that most PEG-grafted bilayers examined experimentally appear to exist in a mushroom-brush transition region that is very broad. If so, our findings suggest that this transition occurs largely in a range of PE-PEG surface densities higher than those examined here.

It is striking to observe that in "snapshot" (instantaneous) views our MC simulations reveal substantial amounts of apparently "free" area on the lipid surface, even at the highest polymer-grafting densities examined. This result might seem to be at variance with our experimental observation that the presence of PE-PEGs at moderate grafting densities can dramatically reduce the affinity of binding of additional polymers (here, acylpeptide-PEG conjugates) to the lipid surface. However, when (as is done in Eqs. 9–11) we take into consideration the mobile nature of the grafted polymer layer (notably the translational freedom of the grafted polymers, which consequently acquire the character of a two-dimensional gas), the strong ability of PEG-lipids to antagonize binding of other macromolecules to lipid surfaces can be readily explained.

Comparison with single-chain mean-field theory for grafted polymers

In our simulations we found that the normalized density profiles $\phi(z)$, the radius-of-gyration profiles $R_{Gx,y}(z)$, and the total energy of the polymer layer remain essentially unchanged, indicating that the polymer chains remain within a mushroom regime, over the full experimental range of grafting densities. This essentially corresponds to the low-density limit of both our previous simulation work (Laradji et al., 1994) and the more recent work of Szleifer and colleagues (Szleifer, 1996; Szleifer and Carignano, 1996). These latter workers examined a system of end-grafted homopolymers via MC simulations of a single polymer in the self-consistent field of the other polymers in the system, including the effect of an excluded volume via an incompressibility condition. This gives strong excluded-volume interactions, which cause the polymers to stretch out considerably, resulting in extended "mushrooms," even at low surface coverage (Szleifer and Carignano, 1996). We also find from our simulations that the polymers can be described as extended mushrooms, although the chains appear somewhat less elongated than found by Szleifer for equivalent grafting densities.

Implications for binding of proteins to PEG-grafted bilayers

The adsorption of proteins to PEG-grafted membranes has been investigated in a few experimental studies (Blume and Cevc, 1993; Torchilin et al., 1994; Harasym et al., 1995; Noppl-Simson and Needham, 1996; Du et al., 1997; Sheth and Leckband, 1997) and by theoretical approaches (Jeon and Andrade, 1991; Jeon et al., 1991) as a function of the polymer structure, size, and grafting density. Noppl-Simson and Needham (1996) reported that the rate of adsorption of streptavidin to vesicles containing biotinyl-lipids decreases exponentially as the content of PE-PEG750 increases. Du et al. (1997) have reported that the extent of binding of several plasma proteins to lipid bilayers declines in a more or less exponential manner as the concentration of bilayer-incorporated PE-PEG5000 increases over the range 0–5 mol%. In cases such as the above, it has typically been found that the rate or extent of protein binding to lipid bilayers is decreased by a large factor (at least 10-fold) when 5–10 mol% PE-PEG is incorporated into the lipid surface.

We can use the formalism applied above to the binding of acylpeptide-PEGs to PE-PEG-containing bilayers (treating the surface-associated macromolecules as components of a van der Waals' gas) to estimate the degree to which incorporation of a PE-PEG into a lipid surface will diminish the affinity of binding of other types of molecules, such as globular proteins. Preliminary simulations of the binding of a spherical 50-kDa protein to a lipid surface containing PE-PEGs suggest that the affinity of protein binding will be reduced by factors on the order of 5-, 30-, and 130-fold, respectively, upon incorporation of 3, 5, or 6 mol% PE-PEG5000 into the lipids. (These estimates were calculated by considering that a spherical protein of the indicated molecular weight, with a hydrated radius of 2.74 nm, would present a cross-sectional area of 17.1 nm^2 at a distance of 1.3 nm from the bilayer surface, a height at which we estimate the monomer density of grafted PEG-5000 chains to be at a maximum (Fig. 7 *B*). We used this cross-sectional area, and estimates of the parameter B derived from direct simulations, together with Eq. 11 to calculate the estimates reported above). These results indicate that the behavior of the simulated systems examined here can account for the dramatic reductions observed in protein binding to PEG-lipid-containing vesicles without the need to postulate that the grafted PEG chains enter the brush regime when present at the densities typically found in "sterically stabilized" liposomes. Instead, the mobile (two-dimensional gas-like)

character of the grafted polymers appears to play a key role in their ability to antagonize the binding of other macromolecules to the lipid surface.

APPENDIX

The following abbreviations are used in the equations described below:

N_F	number of free PEG-conjugates
N_w	number of water molecules
N_G	number of "guest" (acylpeptide-PEG) polymer chains on surface
N_H	number of "host" (PE-PEG) polymer chains on surface
N_L	number of lipid molecules
A_{tot}	total surface area
A_o	total surface area occupied by polymer chains (including clusters of free squares too small to allow binding of a "guest" PEG-conjugate)
A_H	total area covered by "host" (PE-PEG) polymer chains
A_G	total area covered by "guest" (acylpeptide-PEG) polymer chains
a_L	area per lipid molecule
a_H	average area (projected onto the surface plane) per "host" (PE-PEG) polymer chain
a_G	average area per "guest" (acylpeptide-PEG) polymer chain
a_P	average area per "host" and "guest" polymer chain when the chains are of the same size
λ	thermal quantum wavelength
μ_F	total chemical potential for free acylpeptide-PEG conjugates in the aqueous phase
μ_G	total chemical potential for surface-bound ("guest") acylpeptide-PEG conjugates
μ_F^R	reference potential for free acylpeptide-PEG conjugates in the aqueous phase
μ_G^R	reference potential for surface-bound ("guest") acylpeptide-PEG conjugates

Case I: "Host" and "guest" polymers are of the same size

1. Van der Waals gas

The Helmholz free energy $\mathcal{A}_V$ for a binary van der Waals gas (here, the "host" and "guest" polymer chains at the lipid surface) with negligible attractive interactions can be written as

$$\mathcal{A}_V/kT = N_G(\ln(\lambda^2 N_G/(A_{tot} - A_o)) - 1) + N_H(\ln(\lambda^2 N_H/(A_{tot} - A_o)) - 1) \quad (A1)$$

with $A_o = (N_H + N_G) \cdot a_P$. The total chemical potential for the guest PEG conjugate (acylpeptide-PEG) is then given, using Eq. A1, as

$$\mu_G = (\partial \mathcal{A}_V/\partial N_G) + \mu_G^R = kT \ln(N_G\lambda^2/(A_{tot} - A_o)) + kT(A_{tot}/(A_{tot} - A_o)) + \mu_G^R \quad (A2)$$

Similarly, the chemical potential for the free acylpeptide-PEG conjugate in the aqueous phase is given by

$$\mu_F = kT \ln(N_F/N_W) + \mu_F^R \quad (A3)$$

Because the free and surface-bound ("guest") PEG conjugates molecules are in equilibrium, $\mu_G = \mu_F$, and noting that $A_{tot} = N_L a_L$, we obtain

$$\ln(N_G N_W/((N_L N_F) \cdot (\lambda/a_L)^2)) = -\ln(A_{tot}/(A_{tot} - A_o)) - (A_{tot}/(A_{tot} - A_o)) + (\mu_F^R - \mu_G^R)/kT \quad (A4)$$

Because the level of vesicle-bound conjugate molecules bound to the lipid vesicles was <0.2 mol% (and usually much less) in all experiments, we can assume that $N_G \ll N_H$, so that $A_o \approx N_H \cdot a_P$, i.e., the overall coverage of the surface by polymers is ascribable almost exclusively to coverage by the "host" polymer. With this assumption we can make the following approximations:

$$A_{tot}/(A_{tot} - A_o) = A_{tot}/A_{acc} = w \quad (A5)$$

$$A_o/(A_{tot} - A_o) = (A_{tot}/A_{acc}) - 1 = w - 1 \quad (A6)$$

Because the effective dissociation constant $\mathcal{K}_d^o$ for acylpeptide-PEG conjugate binding to a lipid surface without grafted "host" PEG chains is equal to $\exp((\mu_F^R - \mu_G^R)/kT)$, from Eq. A2 the dissociation constant for acylpeptide-PEG binding to the surface containing grafted "host" (PE-) PEG chains is thus given by

$$\mathcal{K}_d = \mathcal{K}_d^o \cdot w \cdot \exp(w - 1) \quad (A7)$$

which is Eq. 9 in the main text.

2. Hard discs (scaled particle theory)

The equation of state for hard discs (scaled particle theory) was given by Helfand et al. (1961) and Henderson (1975) as

$$(p \cdot A_{tot})/(kTN_{HD}) = (1 + y^2/8)/(1 - y)^2 \quad (A8)$$

where p is the pressure, N_{HD} is the number of hard discs, and $y = A_o/A_{tot}$. Considering "host" (PE-PEG) and "guest" (acylpeptide-PEG) polymer chains as a binary mixture of hard discs that are described by Eq. A4, we obtain as the Helmholz free energy

$$\mathcal{A}_{HD}/kT = (N_G + N_H) \cdot 1/8\{-\ln A_{tot} - 7(A_{tot} - A_o) + 9A_o/(A_{tot} - A_o)\} + N_G(\ln(\lambda^2 N_G) - 1) + N_H(\ln(\lambda^2 N_H) - 1) \quad (A9)$$

with $A_o = (N_H + N_G) \cdot a_P$. The chemical potential for the "guest" PEG-conjugates is then

$$\mu_G/kT = \ln(N_G\lambda^2/A_{tot}) + 7/8 \cdot \ln(A_o/(A_{tot} - A_o)) + 1/8(25 + 9A_o/(A_{tot} - A_o)) \cdot A_o/(A_{tot} - A_o) + \mu_G^R/kT \quad (A10)$$

and for the free PEG-conjugates,

$$\mu_F/kT = \ln(N_F/N_W) + \mu_F^R/kT \quad (A11)$$

Using the same principles of the binding equilibrium and the same assumptions as above, we obtain the dissociation constant as

$$\mathcal{K}_d = \mathcal{K}_d^o \cdot w^{7/8} \cdot \exp((9w^2 + 7w - 16)/8) \quad (A12)$$

which leads to Eq. 10 in the main text.

Case II: "Host" and "guest" PEG chains are of different sizes

Van der Waals gas

The ansatz is the same as Eq. A1, with the only difference that the occupied area is now described as $A_o = A_G + A_H = N_G \cdot a_G + N_H \cdot a_H$. The chemical

potential for the surface-bound acylpeptide-PEG conjugate is

$$\mu_G/kT = \ln(N_G\lambda^2/(A_{tot} - A_o)) + (A_G + A_H \cdot a_G/a_H)/(A_{tot} - A_o) + \mu_G^R/kT \quad \text{(A13)}$$

Assuming that for the systems under consideration, $N_G \ll N_H$ and $A_o \approx A_H$, we can write $A_G + A_H \cdot a_G/a_H \approx A_o \cdot a_G/A_H$. With $a_G/a_H = R$, the chemical potential is then given as

$$\mu_G/kT = \ln(N_G\lambda^2/(A_{tot} - A_o)) + R \cdot A_o/(A_{tot} - A_o) + \mu_G^R/kT \quad \text{(A14)}$$

Following the same principles for the binding equilibrium as above, we obtain the dissociation constant:

$$\mathcal{K}_d = \mathcal{K}_d^o \cdot w \cdot \exp(R(w - 1)) \quad \text{(A15)}$$

from which Eq. 11 in the main text is derived.

The authors thank Hong Guo and Ling Miao (Department of Physics, McGill University) for providing their MC simulation program for grafted polymer brushes and for useful discussions, and Sylvie Bilodeau and Robert Mayer (Département de Chimie, Université de Montréal) for performing the NMR measurements.

This work was supported by grants from les Fonds FCAR du Québec to MJZ, ML, and JRS; the National Sciences and Engineering Research Council of Canada to MJZ; the Medical Research Council of Canada to JRS; and by a fellowship award from the Deutsche Forschungsgemeinschaft to SR. MJZ is a fellow of the Canadian Institute of Advanced Research.

REFERENCES

Alexander, S. 1977. Adsorption of chain molecules with a polar head. A scaling description. *J. Physique. (Paris)*. 38:983–987.

Allen, T. M. 1992. Stealth® liposomes: five years on. *J. Liposome Res.* 2:289–305.

Allen, T. M., and L. G. Cleland. 1980. Serum-induced leakage of liposome contents. *Biochim. Biophys. Acta.* 597:418–426.

Allen, T. M., C. Hansen, F. Martin, C. Redemann, and A. Yau-Yong. 1991. Liposomes containing synthetic lipid derivatives of poly(ethylene glycol) show prolonged circulation half-lives in vivo. *Biochim. Biophys. Acta* 1066:29–36.

Baekmark, T. R., S. Pedersen, K. Jorgensen, and O. G. Mouritsen. 1997. The effect of ethylene oxide containing lipopolymers and tri-block copolymers on lipid bilayers of dipalmitoyl-phosphatidylcholine. *Biophys. J.* 73:1479–1491.

Bedu-Addo, F. K., P. Tang, Y. Xu, and L. Huang. 1996. Effects of polyethyleneglycol chain length and phospholipid acyl chain composition on the interaction of polyethyleneglycol-phospholipid conjugates with phospholipid: implications in liposomal drug delivery. *Pharm. Res.* 13:710–717.

Blume, G., and G. Cevc. 1993. Molecular mechanism of the lipid vesicle longevity in vivo. *Biochim. Biophys. Acta.* 1146:157–168.

Bongrand, P. 1988. Physical Basis of Cell-Cell Adhesion. CRC Press, Boca Raton, FL.

Brandrup, J., and E. H. Immergut. 1966. Polymer Handbook. Interscience Publishers, New York.

Cevc, G. 1993. Phospholipids Handbook. Marcel Dekker, New York.

De'Bell, K., and T. Lookman. 1993. Surface phase transitions in polymer systems. *Rev. Mod. Phys.* 65:87–113.

de Gennes, P. G. 1980. Conformations of polymers attached to an interface. *Macromolecules.* 13:1069–1075.

de Gennes, P. G. 1987. Polymers at an interface: a simplified view. *Adv. Colloid Interface Sci.* 27:189–209.

de Gennes, P. G. 1988. Model polymers at interfaces. *In* Physical Basis of Cell-Cell Adhesion. P. Bongrand, editor. CRC Press, Boca Raton, FL. 39–60.

Doi, M., and S. F. Edwards. 1986. The Theory of Polymer Dynamics. Clarendon Press, Oxford.

Du, H., P. Chandaroy, and S. W. Hui. 1997. Grafted poly-(ethylene glycol) on lipid surfaces inhibits protein adsorption and cell adhesion. *Biochim. Biophys. Acta.* 1326:236–248.

Edwards, K., M. Johnsson, G. Karlsson, and M. Silvander. 1997. Effects of polyethyleneglycol-phospholipids on aggregate structure in preparations of small unilamellar liposomes. *Biophys. J.* 73:258–266.

Evans, E., and W. Rawicz. 1997. Elasticity of fuzzy biomembranes. *Phys. Rev. Lett.* 79:2379–2382.

Everaers, R., I. S. Graham, and M. J. Zuckermann. 1995. End-to-end distance distributions and asymptotic behaviour of self-avoiding walks in two and three dimensions. *J. Phys. A Math. Gen.* 28:1271–1288.

Finer, E. G., A. G. Flook, and H. Hauser. 1972. The nature and origin of the NMR spectrum of unsonicated and sonicated aqueous egg yolk lecithin dispersions. *Biochim. Biophys. Acta.* 260:59–69.

Finkelstein, A. V., and J. Janin. 1989. The price of lost freedom: entropy of bimolecular complex formation. *Protein Eng.* 3:1–3.

Flory, P. J., and J. Fisk. 1966. Effect of volume exclusion on the dimensions of polymer chains. *J. Chem. Phys.* 44:2243–2248.

Götter, R., K. Kroy, M. Bärmann, and E. Sackmann. 1996. Dynamic light scattering from semidilute actin solutions: a study of hydrodynamic screening, filament bending stiffness, and the effect of tropomyosin/troponin-binding. *Macromolecules.* 29:30–36.

Gregoriadis, G. 1995. Engineering liposomes for drug delivery: progress and problems. *Trends Biotechnol.* 13:527–537.

Grosberg, A. Y., and A. R. Khokhlov. 1994. Statistical Physics of Macromolecules. AIP Press, New York.

Harasym, T. O., P. Tardi, S. A. Longman, S. M. Ansell, M. B. Bally, P. R. Cullis, and L. S. L. Choi. 1995. Poly(ethylene glycol)-modified phospholipids prevent aggregation during covalent conjugation of proteins to liposomes. *Bioconjug. Chem.* 6:187–194.

Helfand, E., H. L. Frisch, and J. L. Lebowitz. 1961. Theory of the two- and one-dimensional rigid sphere fluids. *J. Chem. Phys.* 34:1037–1042.

Henderson, D. 1975. A simple equation of state for hard discs. *Mol. Phys.* 30:971–972.

Hristova, K., A. K. Kenworthy, and T. J. McIntosh. 1995. Effect of bilayer composition on the phase behavior of liposomal suspensions containing poly(ethylene glycol)-lipids. *Macromolecules.* 28:7693–7699.

Hristova, K., and D. Needham. 1994. The influence of polymer-grafted lipids on the physical properties of lipid bilayers: a theoretical study. *J. Colloid Interface Sci.* 168:302–314.

Hristova, K., and D. Needham. 1995. Phase behavior of a lipid/polymer-lipid mixture in aqueous medium. *Macromolecules.* 28:991–1002.

Huggins, M. L. 1943. Thermodynamic properties of solutions of high polymers: the empirical constant in the activity equation. *Ann. N.Y. Acad. Sci.* 44:431–443.

Iga, K., K. Ohkouchi, Y. Ogawa, and H. Toguchi. 1994. Membrane modification by negatively charged stearyl-polyoxyethylene derivatives for thermosensitive liposomes: reduced liposomal aggregation and avoidance of reticuloendothelial system uptake. *J. Drug Targeting.* 2:259–267.

Janin, J., and C. Chothia. 1978. Role of hydrophobicity in the binding of coenzymes. *Biochemistry.* 17:2943–2948.

Jeon, S. I., and J. D. Andrade. 1991. Protein-surface interactions in the presence of polyethylene oxide. II. Effect of protein size. *J. Colloid Interface Sci.* 142:159–166.

Jeon, S. I., J. H. Lee, J. D. Andrade, and P. G. de Gennes. 1991. Protein-surface interactions in the presence of polyethylene oxide. I. Simplified theory. *J. Colloid Interface Sci.* 142:149–158.

Kenworthy, A. K., K. Hristova, D. Needham, and T. J. McIntosh. 1995a. Range and magnitude of the steric pressure between bilayers containing phospholipids with covalently attached poly(ethylene glycol). *Biophys. J.* 68:1921–1936.

Kenworthy, A. K., S. A. Simon, and T. J. McIntosh. 1995b. Structure and phase behavior of lipid suspensions containing phospholipids with covalently attached poly(ethylene glycol). *Biophys. J.* 68:1903–1920.

Kuhl, T. L., D. E. Leckband, D. D. Lasic, and J. N. Israelachvili. 1994. Modulation of interaction forces between bilayers exposing short-chained ethylene oxide headgroups. *Biophys. J.* 66:1479–1488.

Laradji, M., H. Guo, and M. J. Zuckermann. 1994. Off-lattice Monte Carlo simulation of polymer brushes in good solvents. *Phys. Rev. E.* 49: 3199–3206.

Lasic, D. D. 1995. Applications of liposomes. *In* Handbook of Biological Physics. R. Lipowsky and E. Sackmann, editors. Elsevier Science, Amsterdam. 491–519.

Lasic, D. D., F. J. Martin, A. Gabizon, S. K. Huang, and D. Papahadjopoulos. 1991a. Sterically stabilized liposomes: a hypothesis on the molecular origin of the extended circulation times. *Biochim. Biophys. Acta.* 1070:187–192.

Lasic, D. D., and D. Papahadjopoulos. 1995. Liposomes revisited. *Science.* 267:1275–1276.

Lasic, D. D., M. C. Woodle, F. J. Martin, and T. Valentinčič. 1991b. Phase behavior of "Stealth®-lipid"-lecithin mixtures. *Period. Biol.* 93: 287–290.

Lasic, D. D., M. C. Woodle, and D. Papahadjopoulos. 1992. On the molecular mechanism of steric stabilization of liposomes in biological systems. *J. Liposome Res.* 2:335–353.

Lowry, R. R., and I. J. Tinsley. 1974. A simple, sensitive method for lipid phosphorus. *Lipids.* 9:491–492.

MacDonald, R. C., R. I. MacDonald, B. Ph. M. Menco, K. Takeshita, N. K. Subbarao, and L. Hu. 1991. Small-volume extrusion apparatus for preparation of large, unilamellar vesicles. *Biochim. Biophys. Acta.* 1061: 297–303.

Majewski, J., T. L. Kuhl, M. C. Gerstenberg, J. N. Israelachvili, and G. S. Smith. 1997. Structure of phospholipid monolayers containing poly(ethylene glycol) lipids at the air-water interface. *J. Phys. Chem. B.* 101: 3122–3129.

Martin, F. J., and D. D. Lasic. 1991. The molecular origin of the long blood circulation time of Stealth liposomes. *Biophys. J.* 59:A497 (Abstr.).

Miao, L., H. Guo, and M. J. Zuckermann. 1996. Conformation of polymer brushes under shear: chain tilting and stretching. *Macromolecules.* 29: 2289–2297.

Mori, A., A. L. Klibanov, V. P. Torchilin, and L. Huang. 1991. Influence of the steric barrier activity of amphipathic poly(ethyleneglycol) and ganglioside GM1 on the circulation time of liposomes and on the target binding of immunoliposomes in vivo. *FEBS Lett.* 284:263–266.

Needham, D., N. Stoicheva, and D. V. Zhelev. 1997. Exchange of monooleoylphosphatidylcholine as monomers and micelles with membranes containing poly(ethyleneglycol)-lipid. *Biophys. J.* 73:2615–2629.

Noppl-Simson, D. A., and D. Needham. 1996. Avidin-biotin interactions at vesicle surfaces: adsorption and binding, cross-bridge formation, and lateral interactions. *Biophys. J.* 70:1391–1401.

Nordlund, J. R., C. F. Schmidt, S. N. Dicken, and T. E. Thompson. 1981. Transbilayer distribution of phosphatidylethanolamine in large and small unilamellar vesicles. *Biochemistry.* 20:3237–3241.

Parr, M. J., S. M. Ansell, L. S. Choi, and P. R. Cullis. 1994. Factors influencing the retention and chemical stability of poly(ethylene glycol)-lipid conjugates incorporated into large unilamellar vesicles. *Biochim. Biophys. Acta.* 1195:21–30.

Peitzsch, R. M., and S. McLaughlin. 1993. Binding of peptides and fatty acids to phospholipid vesicles: pertinence to myristoylated proteins. *Biochemistry.* 32:10436–10443.

Sarmoria, C., and D. Blankschtein. 1992. Conformational characteristics of short poly(ethylene oxide) chains terminally attached to a wall and free in aqueous solution. *J. Phys. Chem.* 96:1978–1983.

Sheth, S. R., and D. Leckband. 1997. Measurements of attractive forces between proteins and end-grafted poly(ethylene glycol) chains. *Proc. Natl. Acad. Sci. USA.* 94:8399–8404.

Shahinian, S., and J. Silvius. 1995. Doubly-lipid-anchored protein sequence motifs exhibit long-lived anchorage to lipid bilayers. *Biochemistry.* 34:3813–3822.

Silvius, J. R., and F. l'Heureux. 1994. Fluorimetric evaluation of the affinities of isoprenylated peptides for lipid bilayers. *Biochemistry.* 33:3014–3022.

Silvius, J. R., and M. J. Zuckermann. 1993. Interbilayer transfer of phospholipid-anchored macromolecules via monomer diffusion. *Biochemistry.* 32:3153–3161.

Szleifer, I. 1996. Statistical thermodynamics of polymers near surfaces. *Curr. Opin. Colloid Interface Sci.* 1:416–423.

Szleifer, I., and M. A. Carignano. 1996. Tethered polymer layers. *In* Advances in Chemical Physics, Vol. 44. I. Progogine and S. A. Rice, editors. John Wiley and Sons, New York.

Takahashi, Y., and H. Tadokoro. 1973. Structural studies of polyethers, $(-(CH_2)_m-O-)_n$. X. Crystal structure of poly(ethylene oxide). *Macromolecules.* 6:672–675.

Torchilin, V. P., V. P. Omelyanenko, M. I. Papisov, A. A. Bogdanov, Jr., V. S. Trubetskoy, J. N. Herron, and C. A. Gentry. 1994. Poly(ethylene glycol) on the liposome surface: on the mechanism of polymer-coated liposome longevity. *Biochim. Biophys. Acta.* 1195:11–20.

Woodle, M. C. 1993. Surface-modified liposomes: assessment and characterization for increased stability and prolonged blood circulation. *Chem. Phys. Lipids.* 64:249–262.

Woodle, M. C., L. R. Collins, E. Sponsler, N. Kossovsky, D. Papahadjopoulos, and F. J. Martin. 1992. Sterically stabilized liposomes—reduction in electrophoretic mobility but not electrostatic surface potential. *Biophys. J.* 61:902–910.

Woodle, M. C., and D. D. Lasic. 1992. Sterically stabilized liposomes. *Biochim. Biophys. Acta.* 1113:171–199.

Woodle, M. C., D. D. Lasic, L. R. Collins, T. M. Allen, and F. J. Martin. 1991a. Phase diagram of PEG-DSPE (Stealth® lipid)-egg phosphatidylcholine (EPC) mixtures. *Biophys. J.* 59:A497 (Abstr.).

Woodle, M. C., D. D. Lasic, C. Redemann, M. Newman, S. Babbar, and F. J. Martin. 1991b. In vivo studies of long circulating (Stealth) liposomes in rats. *Period. Biol.* 93:349–352.

Woodle, C. M., M. S. Newman, and P. K. Working. 1995. Biological properties of sterically stabilized liposomes. *In* Stealth Liposomes. D. D. Lasic and F. Martin, editors. CRC Press, Boca Raton, FL. 103–117.